

Local growth rules for an icosahedral substitution tiling

Xuejian Ma and Joshua E. S. Socolar
Physics Department, Duke University, Durham, NC 27708

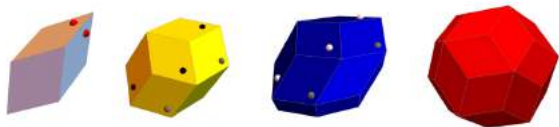


FIG. 1. Four basic tiles (Rhombohedron, Dodecahedron, Icosahedron, and Triacanthedron) with direction marks. The marks on them illustrate how they match each other. The matching rule related to the marks are shown in Fig. 13 at the end of the paper. The pictures are rescaled here to please the eye. The side lengths of the four tiles should be the same in reality.

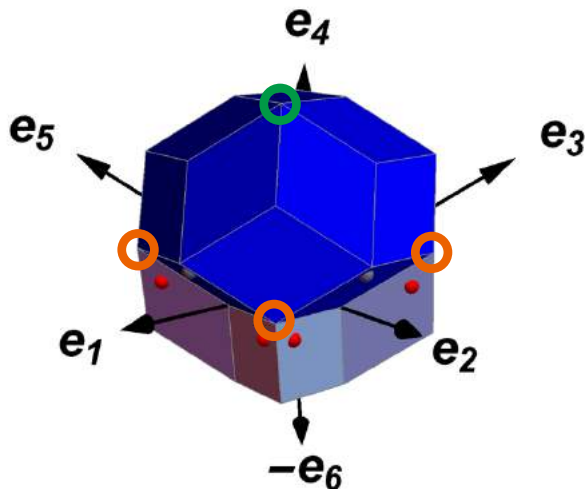


FIG. 2.

I. THE GENERAL GROWTH ALGORITHM

For the Z-tiling, there are four basic tiles: Rhombohedron, Dodecahedron, Icosahedron, and Triacanthedron shown in Figure 1. The mark points on the faces of a tile show how it is oriented and are related to matching rules between tiles shown in Figure 13. A complete vertex is defined as a vertex fully surrounded by several tiles. The possible complete vertex configurations are limited and compiled as Table I. Each row of the table represents a set of tiles fully surrounding a vertex legally.

Let's take row 20 as an example. There are five rhombohedrons and one icosahedron around a vertex, which is the original point here, as shown in Table I. Follow the instructions of Table I and

II, we could construct the configuration shown in Fig. 2. The icosahedron is defined by I_612345 , which means the icosahedron has the starting point $e_1 + e_2 + e_3 + e_4 + e_5$, circled in green. The subscript 6 means the icosahedron is in the 6th direction, $\bar{5}43\bar{2}\bar{1}$, listed in Table II, which means the ending point of the icosahedron should be $e_1 + e_2 + e_3 + e_4 + e_5 + (-e_5) + (-e_4) + (-e_3) + (-e_2) + (-e_1) = \mathbf{0}$, consistent with Fig. 2. Similarly, we could get the starting points for rhombohedrons marked in orange, and the ending point of all rhombohedrons is $-e_6$, also consistent with Fig. 2. Following the same steps, we could rebuild all 27 types of configurations in Table I.

With the discussion above, we define the set formed by the i -th row of Table I as Q_i . In order to grow a cluster from a seed cluster, we need to check the incomplete vertices in the cluster. If we grow from a legal seed, the tiles around an incomplete vertex v form a set $\mathcal{T}(v)$, which must be a subset of one or more Q_i 's, with i as different integers from 1 to 27 representing 27 different types of vertex configurations. The complement of $\mathcal{T}(v)$ in Q_i contains available legal tiles to be added. We define the complement sets as $\mathcal{T}_i(v)$'s. The common tiles in $\mathcal{T}_i(v)$'s are called forced tiles, and they should to be added to $\mathcal{T}(v)$. However, if we grow from an illegal seed, we might encounter some illegal vertices with illegal $\mathcal{T}(v)$, which is not a subset of any Q_i . In this case, we should not consider those illegal vertices during the growing process any more. The vertex we need to check every time should be selected randomly among all legal vertices in the cluster. With the growth of the cluster, there would be more and more vertices and tiles in it. If there's no forced tile in a cluster after the last tile added, the whole cluster would be stuck and stops growing.

II. TWO SPECIAL CASES

Unlike A-tiling, there are two special cases to be considered apart from the general growth algorithm for Z-tiling due to ambiguities in the process of growing. Theoretically, a legal seed could generate a cluster whose growth would stop when it meets the worm planes, which means the final cluster should look like an object with planar "faces" cut by several planes. However, if we grow the cluster only by the general growth algorithm for the Z-tiling, a legal

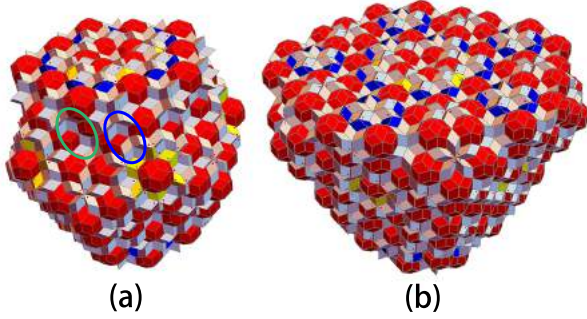


FIG. 3.

seed could result in a weird cluster with "caves" and rough faces outside sometimes as Figure 3 (a) shows. Generally, the "caves" have two basic patterns: the one in the blue circle, and the one in the green circle in Fig. 3 (a). Those two patterns are the two special cases to be discussed below. After solving those two special cases, the cluster would continue growing and finally stops as Figure 3 (b), which is as expected with planar "faces".

In the two special cases, tiles to be added should also be decided by vertices near the reference point apart from it. The following discussion came from the careful observation of the 27 vertex types and the combination of tiles of them. The two special cases could be illustrated in different ways. The following way is a compact, sufficient and necessary one we have.

The tiles in Fig. 4 and Fig. 6 are marked with numbers. One could rebuild those tiles with the help of Table IV.

A. Special case 1

If a vertex has five rhombohedrons and two triacontahedrons around it and the combination of the tiles is the same as Fig. 4(a), where the white point in the middle represents the reference point, we have to consider the two nearby vertices shown as the blue points to determine what kind of tile should be added to the reference point since it is ambiguous currently (it is a subset of both row 21 and row 23 of Table I in certain rotations as Fig. 5 (a)-(b) show).

The way we consider the two blue points is to examine the tiles around them. As shown in Fig. 4(b), if the upper blue vertex has and only has tiles 1, 4, and 8 around it, and the lower blue vertex has and only has tiles 2, 4, and 9, we say the ambiguity would be avoided. In such a case, the combination in Fig. 5(b) would be impossible since it would make the two blue vertices illegal. So the only choice would

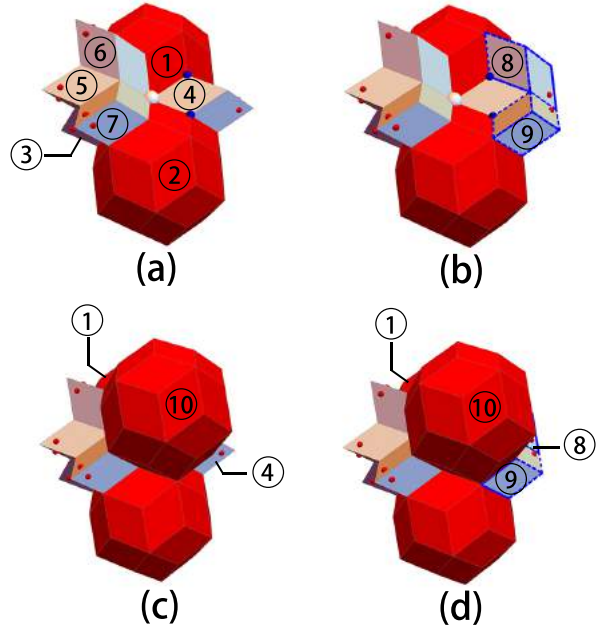


FIG. 4.

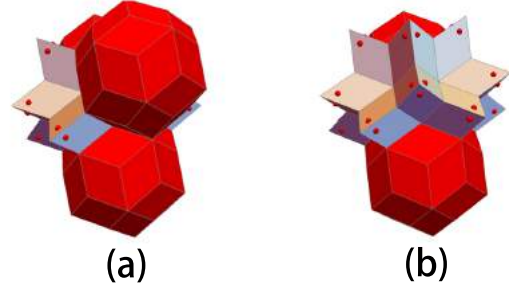


FIG. 5.

be the triacontahedron in Fig. 5(a) and the tile 10 in Fig. 4(d) should be added to the cluster. If we go back and only consider the reference vertex now, the determined tiles around it would form the configuration of Fig. 4(c).

Note that the triacontahedron cannot be added via the general growth algorithm in such a case although it is not ambiguous since we are taking the two nearby vertices into consideration instead of only the reference vertex.

B. Special case 2

The basic methodology of the second special case is similar to the first one. The second case involves a special pattern shown in Fig. 6(a) with two rhombohedrons and two triacontahedrons. The ambiguity occurs here since both row 19 and row 23 in Table

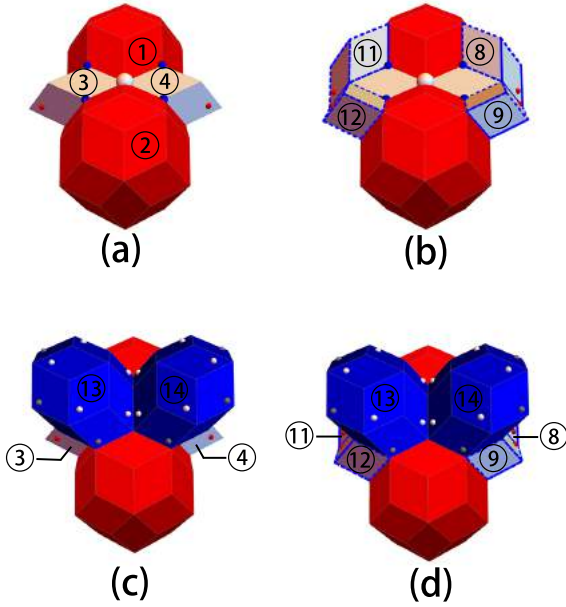


FIG. 6.

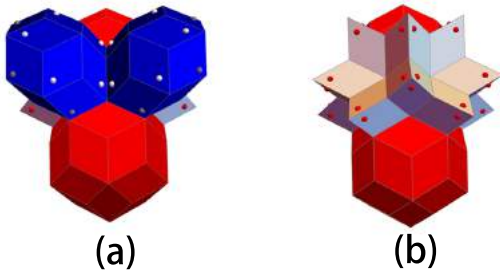


FIG. 7.

IV are possible as Fig. 7(a)-(b) show.

To avoid the ambiguity, we consider the four nearby vertices marked as blue points in Fig. 4(a). If those blue vertices have and only have the tiles 1-4 and tiles 8-12 around them shown in Fig. 4(b), then we say the ambiguity would be avoided since the combination of Fig. 7(b) would make the blue points illegal. The only choice here is to add two icosahedrons in the way shown in Fig. 6(d). If we go back and only consider the reference vertex now, the determined tiles would form the pattern shown in Fig. 6(c).

III. INFINITE SEED

The discovery of the infinite growth of Z-tiling requires an infinite seed. Though Z-tiling and A-tiling share a lot of similarities when it comes to the concept of perp-space and window, the way we find the

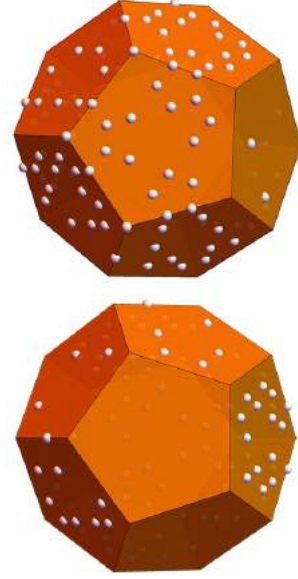


FIG. 8. Perp-space positions of vertices associated with an illegal seed

infinite seed for Z-tiling is quite different from the case in A-tiling due to the increased complexity of configurations. Though we did not find a general way to beget a infinite seed like the work done for A-tiling, we do figure out a particular infinite seed which could help us understand the characteristics of Z-tiling better. The particular case must conform to the common conditions for an infinite seed. The vertices in the perp-space should constrain the location and scale of the perp-space window shown in Fig. 8. The particular seed is generated by dividing the whole space into four regions with different β 's and is shown in Fig. 12(a). The rhombohedrons are neglected since the illegal skinny tiles are incompatible with the illustration system in the growth algorithm and the spaces could be fulfilled during the growing process.

If we grow from the seed, the defects of the cluster would grow approximately linearly which can be seen intuitively in Fig. 9(a). Fig. 9(b) tells us the illegal vertices are constrained in the worm planes intersecting at the original point. By counting the number of illegal vertices during growing process, we get the data shown in Fig. 10, which strongly imply the linear relation between the number of illegal vertices and the one-dimensional scale of the cluster.

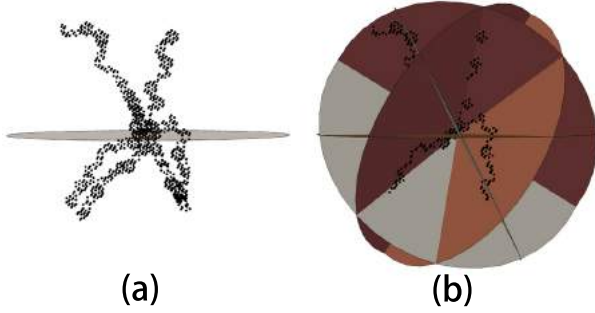
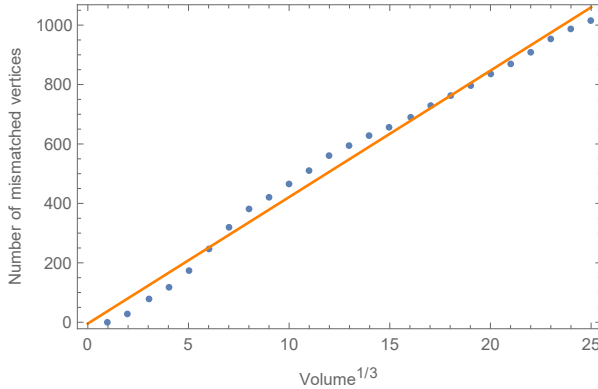


FIG. 9.

FIG. 10. Fitting line in orange: $y = -4.40 + 42.57x$

IV. DISCUSSION

There is a possible way to prove the feasibility of an infinite growth for Z-tiling in general. The legal cluster has the characters of self-similarity and self-inversion. It means that a single tile could be inflated first and then be divided into several compatible matching tiles. On the other hand, particular configurations of tiles could be transformed into one big tile. In other words, we could generate a new legal cluster purely from an old legal cluster by inflating it and dividing it, or finding those particular configurations and transform them into big tiles and deflate the cluster into a smaller one. To make it clear, suppose we have a legal cluster of tiles and those tiles constitute a set C . If we could not find any more forced tile for C , which means it represents a cluster not growing any more by the general growth algorithm with special cases, we could use bigger tiles with the scale factor τ^2 to substitute the original ones by self-similarity rules, and get a new set of tiles, C' . Then we deflate the cluster and acquire a set of regular sized tiles, C'' . C'' must be a subset of C . If C is a set which could not grow further, we can draw the conclusion that C'' could not grow further either, which results in a contradiction if the

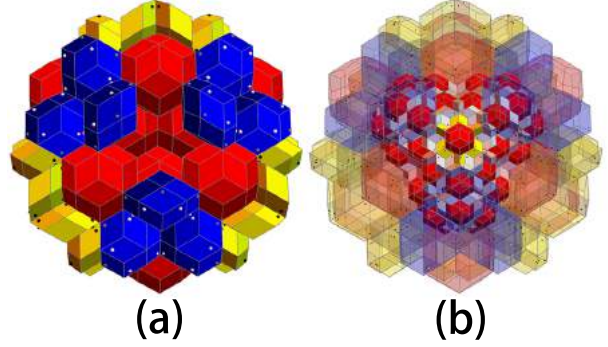


FIG. 11. Legal seed with the stuck cluster. The pictures are rescaled to please the eye

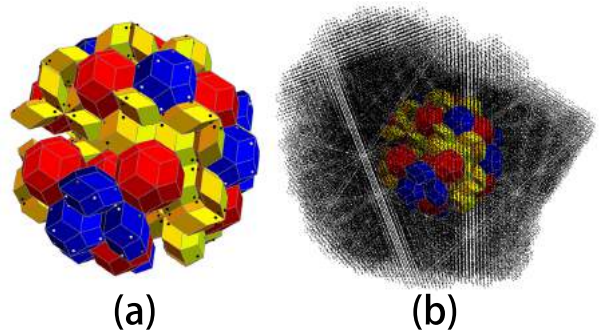


FIG. 12. illegal seed with the stuck cluster. The pictures are rescaled to please the eye

original seed cluster was a subset of C'' . So we have the following claim: in order to grow the cluster into C by the general growth algorithm with special cases, we must start from a seed cluster which contains tiles not belonging to C'' . If we inflate the seed cluster and C'' by τ^2 in the claim above, we could get a new equivalent and more practical claim: in order to grow the cluster into C by the general growth algorithm with special cases, the seed cluster we grow from must have the character that once it was inflated by τ^2 , it should contain tiles not belonging to C' . More intuitively, it means the inflated seed cluster should cover the spaces that C does not cover.

Consider a legal seed shown in Fig. 11(a). The seed could grow to a big stuck cluster shown by the opaque tiles in Fig. 12(b). From our claim above, we can conjecture that after inflating the seed cluster, it would outstrip the range of the stuck cluster. The inflated seed tiles are shown by translucent tiles shown in Fig. 12(b), which obviously verifies our claim.

If we could generalize the claim into a cluster with limited illegal tiles and vertices, we could easily verify whether the illegal seed could generate an infinite cluster or not. Assume the claim was true, then we

need to inflate the illegal seed cluster (Fig. 12(a)) and compare it with the cluster we get till now after we stopped the growth process manually. Since the cluster is huge, we use black dots in Fig. 12(b) to represent the vertices in the cluster to show the position and scale of the big cluster. The seed cluster in Fig. 12(b) was the one after the inflation. It can be seen clearly that the whole inflated seed cluster was completely covered by the huge cluster after the growth. So if the claim for illegal clusters were also true, we could draw the conclusion that there exists an illegal seed that could grow to infinity.

-
- [1] Hans-Rainer Trebin. *Quasicrystals: Structure and Physical Properties*. Wiley-VCH, 2003.

TABLE I. The complete vertex catalog for Z-tiling. Each row represents a unique type of vertex with several particular tiles around it to make it complete. There are 27 types of them regardless of rotations. If one wants to consider rotations, check the comments in Table III. In this table, R, D, I, T represent the tile types: Rhombohedron, Dodecahedron, Icosahedron, and Triacanthedron. The subscript number like 26 in D_{26} is the direction index leading to a particular direction of the tile shown in Table II. The series of numbers after the tile type is the coordinates of the starting point to draw a tile, which is considered as the original point in Table II. The overbars indicate the negative directions. For example, $D_{26}\bar{1}\bar{3}\bar{4}$ indicates that, taking $\mathbf{v}_{start} = -\mathbf{e}_1 - \mathbf{e}_3 - \mathbf{e}_4$ as the starting point for a dodecahedron, we could say that the dodecahedron's vertices are the coordinates of vertices generated by Table II plus \mathbf{v}_{start} .

1	$D_{26}\bar{1}\bar{3}\bar{4}$	$R_4\bar{1}$	$D_7\bar{1}\bar{3}\bar{5}$	$R_8\bar{3}$						
2	$I_5\bar{2}$	$I_8\bar{5}$	$R_7\bar{2}\bar{5}$	$R_6\bar{2}\bar{5}$						
3	$I_5\bar{1}\bar{2}\bar{3}\bar{4}$	$D_{10}\bar{4}$	$R_{16}\bar{1}$	$R_{20}\bar{4}$						
4	$I_5\bar{2}\bar{3}\bar{4}\bar{6}$	$R_{10}\bar{3}$	$R_{16}\bar{6}$	$D_{35}\bar{3}\bar{4}\bar{6}$						
5	$T\bar{1}\bar{2}\bar{3}\bar{4}\bar{6}$	$T\bar{1}$	$R_{14}\bar{2}\bar{4}$	$R_{12}\bar{2}\bar{4}$						
6	$I_6\bar{5}$	$T\bar{1}\bar{4}\bar{5}$	$R_{16}\bar{5}\bar{6}$	$R_{20}\bar{5}\bar{6}$						
7	$I_6\bar{2}\bar{3}\bar{4}\bar{5}$	$R_{17}\bar{2}$	$R_{16}\bar{5}$	$I_1\bar{2}\bar{3}\bar{4}\bar{5}$						
8	$T\bar{1}\bar{2}\bar{3}$	D_{15}	$I_8\bar{1}\bar{3}\bar{6}$	D_5	R_6					
9	$T\bar{1}\bar{2}\bar{3}\bar{4}\bar{6}$	D_{55}	D_{20}	R_8	D_1					
10	$T\bar{2}\bar{3}\bar{6}$	D_{26}	$I_9\bar{1}\bar{4}\bar{6}$	$I_8\bar{1}\bar{4}\bar{6}$	R_7					
11	$D_{30}\bar{1}\bar{2}$	$T\bar{4}$	$R_3\bar{1}\bar{2}$	$R_2\bar{1}\bar{3}$	$R_6\bar{2}\bar{5}$					
12	$I_6\bar{3}\bar{4}\bar{5}$	$T\bar{4}$	R_{17}	$I_2\bar{3}\bar{4}\bar{5}$	$I_1\bar{3}\bar{4}\bar{5}$					
13	$T\bar{1}\bar{2}\bar{5}\bar{6}$	$D_{47}\bar{2}$	$D_{30}\bar{5}$	$D_{42}\bar{4}$	$D_{25}\bar{3}$	$D_9\bar{6}$				
14	$D_{26}\bar{1}\bar{2}\bar{3}$	$T\bar{1}\bar{5}$	$R_{10}\bar{3}$	$D_{27}\bar{3}\bar{4}\bar{5}$	$R_8\bar{3}$	$R_9\bar{3}$				
15	$I_{12}\bar{1}\bar{2}$	$T\bar{2}\bar{3}\bar{4}\bar{6}$	$D_{26}\bar{4}$	$R_4\bar{1}\bar{2}\bar{6}$	$I_8\bar{1}\bar{6}$	$D_7\bar{5}$				
16	$D_{30}\bar{1}\bar{2}\bar{3}$	$T\bar{3}\bar{4}$	$R_3\bar{1}$	$R_4\bar{1}$	$R_2\bar{1}$	$R_5\bar{1}$				
17	$T\bar{1}\bar{2}$	$R_{14}\bar{4}$	$R_{11}\bar{4}$	$R_{12}\bar{4}$	$R_9\bar{4}$	$R_{13}\bar{4}$				
18	I_6	$R_{17}\bar{6}$	$R_{16}\bar{6}$	$R_{18}\bar{6}$	$R_{19}\bar{6}$	$R_{20}\bar{6}$				
19	$I_6\bar{4}\bar{5}$	$T\bar{1}\bar{5}$	$T\bar{3}\bar{4}$	$I_2\bar{4}\bar{5}$	$R_{12}\bar{2}\bar{4}\bar{5}$	$R_{20}\bar{4}\bar{5}\bar{6}$				
20	$I_6\bar{1}\bar{2}\bar{3}\bar{4}\bar{5}$	$R_{17}\bar{1}\bar{2}$	$R_{16}\bar{1}\bar{5}$	$R_{18}\bar{2}\bar{3}$	$R_{19}\bar{3}\bar{4}$	$R_{20}\bar{4}\bar{5}$				
21	$T\bar{1}\bar{4}\bar{5}\bar{6}$	$T\bar{2}\bar{3}\bar{4}\bar{6}$	T	$R_3\bar{1}\bar{2}\bar{4}$	$R_{14}\bar{1}\bar{2}\bar{4}$	$R_4\bar{1}\bar{2}\bar{6}$	$R_2\bar{1}\bar{3}\bar{4}$	$R_6\bar{2}\bar{4}\bar{5}$		
22	$I_5\bar{2}\bar{3}\bar{4}$	$D_{26}\bar{3}\bar{4}$	R_4	$D_{10}\bar{1}\bar{4}$	$I_8\bar{3}\bar{4}\bar{5}$	R_{16}	$D_{51}\bar{4}\bar{6}$	R_7	R_6	$D_{35}\bar{3}\bar{4}$
23	$T\bar{1}\bar{5}$	$T\bar{3}\bar{4}$	$R_3\bar{1}\bar{2}\bar{4}$	$R_4\bar{1}\bar{2}\bar{6}$	$R_5\bar{1}\bar{5}\bar{6}$	$R_7\bar{2}\bar{3}\bar{5}$	$R_8\bar{2}\bar{3}\bar{6}$	$R_6\bar{2}\bar{4}\bar{5}$	$R_{12}\bar{2}\bar{4}\bar{5}$	$R_9\bar{3}\bar{4}\bar{6}$
	$R_{13}\bar{4}\bar{5}\bar{6}$	$R_{20}\bar{4}\bar{5}\bar{6}$								
24	$D_{26}\bar{1}\bar{2}$	$D_{30}\bar{2}\bar{3}$	R_3	$D_{15}\bar{2}\bar{6}$	R_4	R_2	R_{10}	R_5	$D_{51}\bar{2}\bar{3}$	R_7
	R_8	$D_1\bar{2}\bar{4}$	R_6	R_9	R_{20}					
25	$T\bar{4}\bar{5}$	$R_3\bar{1}\bar{2}\bar{4}$	$R_4\bar{1}\bar{2}\bar{6}$	$R_2\bar{1}\bar{3}\bar{4}$	$R_{11}\bar{1}\bar{3}\bar{4}$	$R_1\bar{1}\bar{3}\bar{5}$	$R_{10}\bar{1}\bar{3}\bar{5}$	$R_5\bar{1}\bar{5}\bar{6}$	$R_{16}\bar{1}\bar{5}\bar{6}$	$R_7\bar{2}\bar{3}\bar{5}$
	$R_8\bar{2}\bar{3}\bar{6}$	$R_6\bar{2}\bar{4}\bar{5}$	$R_9\bar{3}\bar{4}\bar{6}$	$R_{19}\bar{3}\bar{4}\bar{6}$	$R_{13}\bar{4}\bar{5}\bar{6}$	$R_{20}\bar{4}\bar{5}\bar{6}$				
26	R_{14}	R_3	R_{17}	R_4	R_{11}	R_2	R_{10}	R_1	R_{16}	R_5
	R_{15}	R_7	R_{18}	R_8	R_{12}	R_6	R_{19}	R_9	R_{20}	R_{13}
27	$R_3\bar{1}\bar{2}\bar{4}$	$R_{14}\bar{1}\bar{2}\bar{4}$	$R_4\bar{1}\bar{2}\bar{6}$	$R_{17}\bar{1}\bar{2}\bar{6}$	$R_2\bar{1}\bar{3}\bar{4}$	$R_{11}\bar{1}\bar{3}\bar{4}$	$R_1\bar{1}\bar{3}\bar{5}$	$R_{10}\bar{1}\bar{3}\bar{5}$	$R_5\bar{1}\bar{5}\bar{6}$	$R_{16}\bar{1}\bar{5}\bar{6}$
	$R_7\bar{2}\bar{3}\bar{5}$	$R_{15}\bar{2}\bar{3}\bar{5}$	$R_8\bar{2}\bar{3}\bar{6}$	$R_{18}\bar{2}\bar{3}\bar{6}$	$R_6\bar{2}\bar{4}\bar{5}$	$R_{12}\bar{2}\bar{4}\bar{5}$	$R_9\bar{3}\bar{4}\bar{6}$	$R_{19}\bar{3}\bar{4}\bar{6}$	$R_{13}\bar{4}\bar{5}\bar{6}$	$R_{20}\bar{4}\bar{5}\bar{6}$

TABLE II. Table of tiles in different directions. For a type of tiles, each number before a colon in the table is the direction index, and the numbers following the colon indicate the direction of the tile. From those numbers, we could get all the vertices for the tile. For a rhombohedron, if the numbers are abc , then the vertices of it would be: $\mathbf{0}, e_a, e_b, e_c, e_a + e_b, e_b + e_c, e_c + e_a, e_a + e_b + e_c$, where $\mathbf{0}$ is the starting point of the tile. To make it easier to read, we write it in the form: $\mathbf{0}, a, b, c, ab, bc, ca, abc$. For a dodecahedron, if the numbers are $abcd$, the vertices would be: $\mathbf{0}, a, b, c, d, ab, bc, cd, da, abc, bcd, cda, dab, abcd$. For an icosahedron, if the numbers are $abcde$, the vertices would be: $\mathbf{0}, a, b, c, d, e, ab, bc, cd, de, ea, abc, bcd, cde, dea, eab, abcd, bcda, cdea, deab, eabc, abcde$. For a triacontahedron, if the numbers are $abcdef$, the vertices would be: $\mathbf{0}, a, b, c, d, e, ab, bc, cd, de, ea, abc, bcd, cde, dea, eab, abf, bcf, cdf, def, eaf, abcf, bcdf, cdef, deaf, eabf, abcdf, bcdef, cdeaf, deabf, eabcf, abcdef$. According to Table III, there are 60 directions for each type of tiles originally. However, due to the rhombohedron's threefold symmetry, it only has 20 different directions. The icosahedron has 12 different directions due to its fivefold symmetry. Although the dodecahedron has twofold symmetry generally, it has no symmetry for the starting point we pick. Though the triacontahedron only has the fivefold symmetry if we pick a vertex as its starting point, we did some manipulation in generating Table I such that the starting point would always be the vertex with the minimum coordinate in the z-direction. So we only need one triacontahedron direction (upward) to construct the structure.

R	1 : 5 $\bar{3}$ 1	2 : 3 $\bar{4}$ 1	3 : 4 $\bar{2}$ 1	4 : 261	5 : 651	6 : 4 $\bar{5}$ 2	7 : 5 $\bar{3}$ 2	8 : 362	9 : 463	10 : 5 $\bar{1}$ 3
	11 : 1 $\bar{4}$ 3	12 : 2 $\bar{5}$ 4	13 : 564	14 : 1 $\bar{2}$ 4	15 : 2 $\bar{3}$ 5	16 : 5 $\bar{6}$ 1	17 : 6 $\bar{2}$ 1	18 : 6 $\bar{3}$ 2	19 : 6 $\bar{4}$ 3	20 : 6 $\bar{5}$ 4
D	1 : 4 $\bar{2}$ 65	2 : 265 $\bar{3}$	3 : 65 $\bar{3}$ 4	4 : 5 $\bar{3}$ 42	5 : 3 $\bar{4}$ 26	6 : 4 $\bar{5}$ 36	7 : 5 $\bar{3}$ 61	8 : 361 $\bar{4}$	9 : 614 $\bar{5}$	10 : 14 $\bar{5}$ 3
	11 : 2 $\bar{5}$ 14	12 : 5 $\bar{1}$ 46	13 : 1 $\bar{4}$ 62	14 : 462 $\bar{5}$	15 : 62 $\bar{5}$ 1	16 : 63 $\bar{1}$ 2	17 : 3 $\bar{1}$ 2 $\bar{5}$	18 : 1 $\bar{2}$ 56	19 : 2 $\bar{5}$ 63	20 : 563 $\bar{1}$
	21 : 164 $\bar{2}$	22 : 642 $\bar{3}$	23 : 42 $\bar{3}$ 1	24 : 2 $\bar{3}$ 16	25 : 3 $\bar{1}$ 64	26 : 1234	27 : 2345	28 : 3451	29 : 4512	30 : 5123
	31 : 3 $\bar{5}$ 6 $\bar{2}$	32 : 5 $\bar{6}$ 24	33 : 6 $\bar{2}$ 43	34 : 243 $\bar{5}$	35 : 435 $\bar{6}$	36 : 1 $\bar{6}$ 3 $\bar{5}$	37 : 6 $\bar{3}$ 54	38 : 3 $\bar{5}$ 4 $\bar{1}$	39 : 541 $\bar{6}$	40 : 41 $\bar{6}$ 3
	41 : 641 $\bar{5}$	42 : 415 $\bar{2}$	43 : 152 $\bar{6}$	44 : 526 $\bar{4}$	45 : 264 $\bar{1}$	46 : 521 $\bar{3}$	47 : 213 $\bar{6}$	48 : 136 $\bar{5}$	49 : 365 $\bar{2}$	50 : 652 $\bar{1}$
	51 : 324 $\bar{6}$	52 : 246 $\bar{1}$	53 : 461 $\bar{3}$	54 : 613 $\bar{2}$	55 : 132 $\bar{4}$	56 : 543 $\bar{2}$	57 : 432 $\bar{1}$	58 : 321 $\bar{5}$	59 : 215 $\bar{4}$	60 : 154 $\bar{3}$
I	1 : 356 $\bar{2}$ 4	2 : 163 $\bar{5}$ 4	3 : 6415 $\bar{2}$	4 : 5213 $\bar{6}$	5 : 3246 $\bar{1}$	6 : 5432 $\bar{1}$	7 : 4265 $\bar{3}$	8 : 45361	9 : 25146	10 : 6312 $\bar{5}$
	11 : 1642 $\bar{3}$	12 : 12345								
T	123456									

TABLE III. Table of rotation vectors. Table I of the 27 types of complete vertices does not show all possible directions. Each tile configuration of the 27 rows in Table I can be rotated by particular angles and get congruent configurations of tiles. In order to get all possible types of complete vertices with consideration of directions, we generate the table of rotation vectors as below. Both Table I and Table II should be converted by Table III to figure out all direction choices. The way to do it is to change all the numbers representing vectors and directions (not including direction indices in Table II) according to the numbers in Table III. For example, if we want to rotate the cluster by 234516 in Table III, we need to change 1, 2, 3, 4, 5, 6 into 2, 3, 4, 5, 1, 6 for all numbers in two tables above, which means $D_{26}1\bar{3}4$ in Table I would be redefined as $D_{26}2\bar{4}5$, and $D : 26 : 1234$ in Table II would be changed into $D : 26 : 2345$. Following those steps and one could get all possible complete vertices taking directions into consideration. For sure some cases would have duplicate configurations under certain rotations due to symmetry.

123456	234516	345126	451236	512346	4265 $\bar{3}$ 1	265 $\bar{3}$ 41	65 $\bar{3}$ 421	534261	342651	453612	536142
361452	614532	145362	251463	514623	1462 $\bar{5}$ 3	462 $\bar{5}$ 13	625 $\bar{1}$ 43	631254	312564	125634	256314
563124	164235	642315	423165	231645	316425	356241	562431	624351	243561	435621	163542
635412	354162	541632	416352	641523	415263	152643	526413	264153	521364	213654	136524
365214	652134	324615	246135	461325	613245	132465	543216	432156	321546	215436	154326

TABLE IV. Table of tiles of special cases. The tiles can be drawn in the same way as Table I.

1 : $T\bar{3}4$	2 : $T\bar{1}456$	3 : $R_{18}236$	4 : $R_9\bar{3}46$	5 : $R_{19}346$	6 : $R_{20}456$	7 : $R_2\bar{1}34$
8 : $R_{13}\bar{3}46$	9 : $R_{11}\bar{3}46$	10 : $T\bar{1}236$	11 : $R_{15}236$	12 : $R_{17}236$	13 : I_236	14 : $I_{10}\bar{3}6$

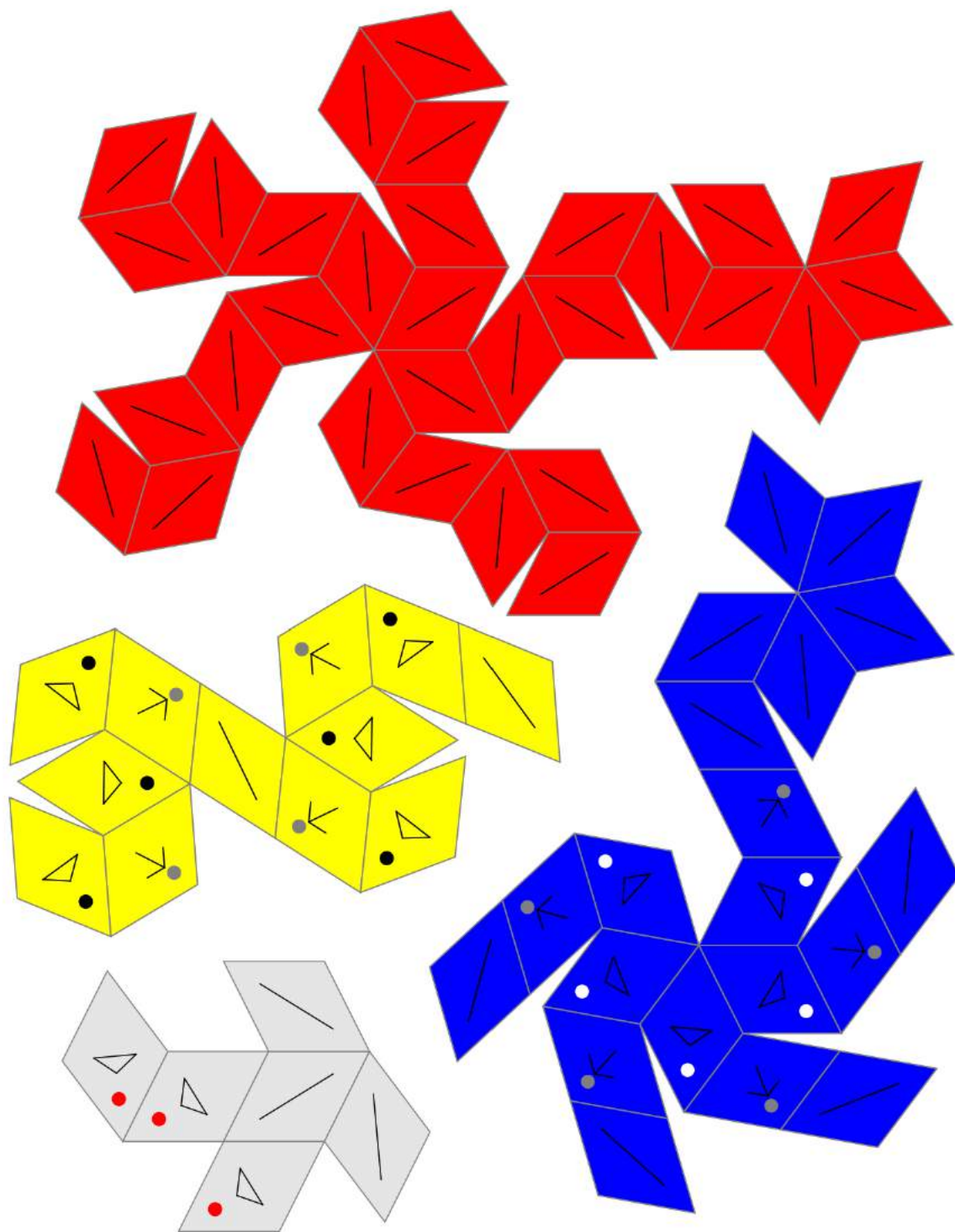


FIG. 13. Matching rule decoration for the unit cells of the PLI class packing.